[CANCER RESEARCH 58, 5023–5026, November 15, 1998]

Advances in Brief

Refined Chromosomal Localization of the Mismatch Repair and Hereditary Nonpolyposis Colorectal Cancer Genes *hMSH2* and *hMSH6*[1]

Christoph Schmutte, Rodica Catrinel Marinescu, Neal G. Copeland, Nancy A. Jenkins, Joan Overhauser, and Richard Fishel[2]

Kimmel Cancer Center, Thomas Jefferson University, Philadelphia, Pennsylvania 19107 [C. S., R. C. M., J. O., R. F.]; and Mammalian Genetics Laboratory, ABL-Basic Research Program, National Cancer Institute-Frederick Cancer Research and Development Center, Frederick, Maryland 21702 [N. G. C., N. A. J.]

Abstract

The genomic loci for the mismatch repair genes *hMSH2* and *hMSH6* were mapped by fluorescence *in situ* hybridization, analysis of radiation hybrid panel markers, and linkage analysis of syntenic chromosome regions between human and mouse. Both genes were localized to chromosome 2p21, adjacent to the luteinizing hormone/choriogonadotropin receptor gene (*LHCGR*; 2p21), telomeric to the D2S123 polymorphic marker, and centromeric to the calmodulin-2 gene (*CALM-2*; 2p22–21) and son-of-sevenless gene (*SOS*; 2p22–21). The genomic locations of *hMSH2* and *hMSH6* appears to be within 1 Mb of each other because they could not be separated by interphase fluorescence *in situ* hybridization. These results clarify the position of the chromosome 2 hereditary nonpolyposis colorectal cancer locus, which was originally reported to be associated with an adjacent region (chromosome 2p14–16).

Introduction

Mismatched DNA bases arise in DNA during the DNA replication process, from chemical and physical nucleotide damage such as hydrolytic deamination of 5-methylcytosine to thymine, and from recombination of DNA derived from different parental DNA sequences (1–3). These mismatches must be repaired to prevent the formation of mutations during the next replication cycle. In the *Escherichia coli* postreplication MMR[3] process, the MutS protein has been shown to initiate repair by binding mismatched nucleotides as homodimers (4). The reaction is then completed by excision and resynthesis of the DNA strand containing the mismatched nucleotide, which requires MutL, MutH, DNA helicase II [uvrD(mutU)], an exonuclease, and the Pol III holoenzyme complex (5). Inactivating mutations of *mutH*, *mutL*, *mutS*, and *uvrD(mutU)* abolish MMR and lead to a mutator phenotype (6–10).

MutS homologues have been found in nearly all species examined, confirming their high conservation throughout evolution (for a recent review, see Ref. 11). Several of these proteins have been found to form heterodimers, which recognize a wide variety of mismatched nucleotides: MSH2-MSH6 binds preferentially to single-base mismatches, whereas MSH2-MSH3 prefers extrahelical mismatched nucleotides (12–14). The central role of hMSH2 (15) and, thus, MMR in maintaining the integrity of DNA is accentuated by the finding that it is frequently inactivated in the cancer susceptibility syndrome HNPCC, many types of sporadic tumors, and tumor-derived cell lines (16). Because the polymerase errors typical of postreplication MMR defects often occur at repeated sequences, such tumors are often characterized by a simple repeat instability or MSI phenotype (17–20). Thus, >90% of all tumors from HNPCC patients that inherit a germ-line mutation in one of the MMR genes display MSI (21). Interestingly, germ-line mutations of the MMR genes are largely confined to *hMSH2* (46%) and the human *mutL* homologue *hMLH1* (48%; Ref. 16).

The human MMR gene, *hMSH2*, was first identified in 1993 (15). At that time, the mouse homologue *Msh2* was mapped to a region of chromosome 17, which displayed synteny with the human chromosome 2p22–21 (15). This mouse mapping and synteny data were supported by the observation that a fragment of *hMSH2* could be amplified using human chromosome 2 genomic DNA as template (15). Interestingly, linkage analysis by Peltomäki *et al.* (22) had localized the HNPCC locus to D2S123 on chromosome 2p16–15. In their confirmatory report following the identification of *hMSH2* (15), Leach *et al.* (23) further defined the *hMSH2* genomic locus using a genomic clone containing 85 kb surrounding *D2S123*, additional markers derived from human P1 and yeast artificial chromosome libraries, and markers derived from chromosome 2p16 microdissection for "fiber" FISH. They reported the physical location of the *hMSH2* gene to be on chromosome 2p16 between marker D2S288 and marker CA5. The latter has not been characterized further. The idea that *hMSH2* may be more distal on chromosome 2 than originally proposed by Vogelstein and colleagues (23) was underscored by the linkage analysis of seven Canadian HNPCC families, which suggested that the HNPCC locus resided telomeric to the marker D2S123 and centromeric to D2S391 (24). Although numerous mutations in the *hMSH2* gene have confirmed its association with the HNPCC phenotype (16), these results clearly defined conflicting mapping data that have confounded the literature.

In this study, we have refined the *hMSH2* and *hMSH6* map positions using high-resolution chromosomal FISH and RH mapping analysis of human chromosomes and compared this data to mouse mapping studies of syntenic chromosome regions. Taken together, the results suggest *hMSH2* is located on chromosome 2p21 and *hMSH6* is located on chromosome 2p21–16.3. Because none of the markers used by Leach *et al.* (23) had been localized relative to the RH grid, we also mapped several of the relevant genes and markers at chromosome 2p22–16. These studies have placed *hMSH2* and *hMSH6* in a tight framework of markers that will be useful for further studies of this genomic locus in human tumors. In addition, we have localized *Msh6* in the mouse to complete the description of the *Msh2/Msh6* locus.

Materials and Methods

Mapping by RH Method. The following primers were used in PCRs to screen the Genebridge-4 Radiation Hybrid Panel (Version RH02.02; Research Genetics, Inc.; Ref. 25): *hMSH2* (x155, 5′-TGT-AAA-ACG-ACG-GCC-AGT-

Received 7/31/98; accepted 10/1/98.

The costs of publication of this article were defrayed in part by the payment of page charges. This article must therefore be hereby marked *advertisement* in accordance with 18 U.S.C. Section 1734 solely to indicate this fact.

[1] This work was supported by NIH Grants CA56542 and CA57007. This research was supported, in part, by the National Cancer Institute, Department of Health and Human Services, under contract with ABL.

[2] To whom requests for reprints should be addressed, at Kimmel Cancer Center, 233 South 10th Street, Room 933, Philadelphia, PA 19107. Phone: (213) 503-1345; Fax: (215) 923-1098; E-mail: rfishel@hendrix.jci.tju.edu.

[3] The abbreviations used are: MMR, mismatch repair; MSH, *mutS* homologue; HNPCC, hereditary nonpolyposis colorectal cancer; MSI, microsatellite instability; FISH, fluorescence *in situ* hybridization; RH, radiation hybrid.

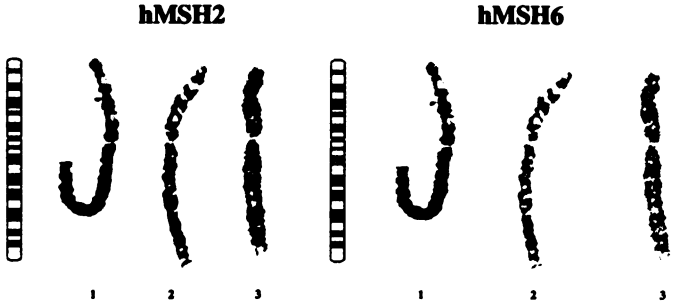

Fig. 1. FISH analysis. Metaphase nuclei were stained as described in "Materials and Methods." Chromosomes 2 from three different metaphase nuclei were aligned (*1–3*). Biotin-14 dATP was used to label the *hMSH2* probe (*green, left*), and digoxygenin-II-dUTP was used to label the *hMSH6* probe (*red, right*). Both signals are confined to 2p21–16.3.

AGG-CGG-GAA-ACA-GCT-TAG-3′/x156, 5′-AAA-GGA-GCC-GCG-CCACAA-3′); *hMSH6* (x306, 5′-CAT-TCA-CAG-GCT-GGC-TTA-TTA-GC-3′/x308, 5′-TCT-GTC-TGA-GGC-ACC-AAG-TCT-3′); D2S123 (x163, 5′-AAA-CAG-GAT-GCC-TGC-CTT-TA-3′/x164, 5′-GGA-CTT-TCC-ACC-TAT-GGG-AC-3′); D2S391 (x165, 5′-ATG-GAG-CCA-GTA-GGT-TAC-AGC-3′/x166, 5′-GGT-GAG-AGG-GTA-TGA-TGG-AA-3′); *LHCGR* (x311, 5′-CTC-AAT-GGC-TAC-GTG-TGA-CTA-G-3′/x312, 5′-CGA-GGA-GTT-TAC-AGT-CTA-CAG-CTT-3′); *CALM2* (x161, 5′-TCA-GTA-ACA-TGT-TGC-ATG-TGG-3′/x162, 5′-AAA-GGC-ATA-ACC-CAG-ATG-TTC-3′); and D2S288 (x281, 5′-GTT-AGG-GCC-TTG-CTC-TGG-AT-3′/x282, 5′-CTA-CAG-TGG-GCT-CTA-TGT-GTT-C-3′). Fragments were visualized by agarose gel electrophoresis, and data were submitted to the Whitehead Institute/MIT Center for Genome Research (http://www.genome.wi.omit.edu) for final analysis.

FISH. FISH was performed using normal peripheral blood lymphocytes in metaphase and interphase, respectively. Cells were fixed onto microscope slides and denatured at 70°C in 70% formamide, followed by sequential dehydration in 70, 80, and 95% ethanol. DNA from P1 clones (a generous gift from Dr. R. Kolodner, University of California, San Diego, La Jolla, CA) containing either *hMSH2* gene (exons 2–16) or *hMSH6* gene (exons 2–10) were sonicated for 15 s and labeled by nick translation with biotin-14 dATP (*hMSH2*) or digoxygenin-II-dUTP (*hMSH6*), respectively, using the BioNick Labeling Kit (BRL, Gaithersburg, MD). A total of 200 ng of each labeled DNA probe, 6 μg of unlabeled human Cot-1 DNA (BRL), and 1.5 μg of sonicated salmon sperm DNA were resuspended in 10 μl of hybridization solution containing 50% formamide, 10% dextran sulfate, and 1× SSC. The probe was denatured at 70°C for 8 min prior to adding the solution to the slide. Hybridization was performed at 37°C for 16 h. Subsequently, the slides were washed twice in 0.5× SSC at 70°C for 2.5 min and once in 4× SSC at room temperature for 2 min. After incubation in a solution containing 1% BSA and 4× SSC at room temperature for 5 min, the probe was detected immunologically using 10 μg/ml FITC conjugated to avidin (FITC-avidin DCS; Molecular Probes, Eugene, OR), 2 μg/ml rhodamine (Boehringer Mannheim, Indianapolis, IN) in 1% BSA, and 4× SSC at 37°C for 30 min. The chromosomes were counterstained with 200 ng/ml 4,6-diamidino-2-phenylindole dihydrochloride in a standard antifade solution. The evaluation was performed using a Nikon Labophot microscope. Images were taken using a cooled charge-coupled device camera (Princeton Instruments, Trenton, NJ). Image processing was performed with PSI software (Perceptive Scientific Instruments, League City, TX).

Interspecific Mouse Backcross Mapping. Interspecific backcross progeny were generated by mating (C57BL/6J × *Mus spretus*)F_1 females and C57BL/6J males as described (26). A total of 205 N_2 mice were used to map the *Msh6* locus. DNA isolation, restriction enzyme digestion, agarose gel electrophoresis, Southern blot transfer, and hybridization were performed essentially as described (27). All blots were prepared with Hybond-N^+ nylon membrane (Amersham). The probe, an ~2.6-kb *NotI/PstI* fragment of human cDNA, was labeled with [α-^{32}P]dCTP using a random primed labeling kit (Stratagene); washing was performed to a final stringency of 1.0× SSC-0.1% SDS at 65°C. Major fragments of 7.6, 3.0, 1.4, 1.2, and 0.06 kb were detected in *TaqI*-digested C57BL/6J DNA, and major fragments of 5.4, 2.7, 2.5, and 0.6 kb were detected in *TaqI*-digested *M. spretus* DNA. The presence or absence of the *TaqI M. spretus*-specific fragment was followed in backcross mice. The 5.4- and 2.5-kb fragments cosegregated, mapped to mouse chromosome 17, and defined *Msh6*. The 2.7-kb *TaqI M. spretus*-specific fragment mapped to mouse chromosome 4.

A description of the probes and RFLPs for the loci linked to *Msh6*, including *Tik*, *Sos1*, *Msh2*, and *Lhcgr*, has been reported previously (15). Recombination distances were calculated using Map Manager Version 2.6.5. Gene order was determined by minimizing the number of recombination events required to explain the allele distribution patterns.

Results and Discussion

FISH Analysis of hMSH2 and hMSH6. To characterize the human *hMSH2* and *hMSH6* genomic loci, we performed high-resolution chromosomal FISH analysis using DNA from P1 clones containing the *hMSH2* exons 2–16 and DNA from P1 clones containing the *hMSH6* exons 2–10. Both *hMSH2* (green) and *hMSH6* (red) appear to be located at chromosome 2p21 at the border region to 2p16.3 (Fig. 1), with the indicative dark banding pattern of the 2p16 region clearly visible in all chromosomes as centromeric to the hMSH2/hMSH6 fluorescence signal. Furthermore, the FISH signals of both *hMSH2* and *hMSH6* appear largely superimposed, even in interphase nuclei, indicating that the genomic loci of these genes are very close (Fig. 2).

RH Examination of Human Chromosome 2p22–16. To substantiate these chromosomal FISH results, we performed RH analysis using primers that were specific for *hMSH2* exon 1 and *hMSH6* exon 6, respectively (Fig. 3). Mapping data returned by the Whitehead Institute/MIT Center for Genome Research indicated that the *hMSH2* gene was 2.3 cR centromeric to marker WI-3220 and 4.3 cR telomeric to marker WI-4108. Similarly, the genomic locus of *hMSH6* was found to be 4.4 cR centromeric to marker WI-4108 and 3.6 cR telomeric to marker WI-3027 (Fig. 3). Assuming 270 kb per cR (28, 29), the distance between these *hMSH2* and *hMSH6* was calculated to be ~2.2 Mb. However, it should be noted that the average resolution of the RH panel is likely to be no greater than 1 Mb. Furthermore, this analysis should be compared to that of Papadopoulos *et al.* (30), who found that both *hMSH2* and *hMSH6* genes were contained on the single yeast artificial chromosome (5A11) DNA. Thus, it is possible that the distance between both genes is less than the RH calculation of 2.2 Mb and is, perhaps, on the order of 1 Mb.

To further pinpoint the hMSH2 genomic location, we determined the chromosomal locations of the calmodulin-2 gene (*CALM2*) and luteinizing hormone/choriogonadotropin receptor gene (*LHCGR*) by RH analysis. *CALM2* has been previously mapped by FISH to 2p22–21 (31). This localization is consistent with our RH data, which suggests that *CALM2* is 12.5 cR centromeric to marker WI-3742 or ~20 Mb telomeric to *hMSH2* (Fig. 3). *LHCGR* was previously mapped by FISH to chromosome 2p21 (32). Interestingly, the RH analysis placed this gene 1.6 cR centromeric to marker WI-4108, between *hMSH2* (6.1 cR centromeric) and *hMSH6* (2.0 cR telomeric). Marker D2S123 had been used by Peltomäki *et al.* (22) to determine the HNPCC locus by linkage analysis, and Leach *et al.* (23) had mapped it to 2p16 by FISH. We determined that D2S123 was 3.56 cR centromeric to marker WI-3027 or 12.3 cR centromeric to *hMSH2*. Similar analysis indicated that the D2S288 and D2S391 markers were indistinguishable from the map location of *hMSH2*, which was found to be telomeric to *hMSH6* (Fig. 3). These latter findings confirm the report of Leach, *et al.*, who showed that the *hMSH2* gene is located near D2S288 (23). However, our data and the reported mapping position of *LHCGR* to 2p21 suggest that both D2S288 and the hMSH2 genomic locus reside at chromosome 2p21, which is more telomeric than reported originally (23).

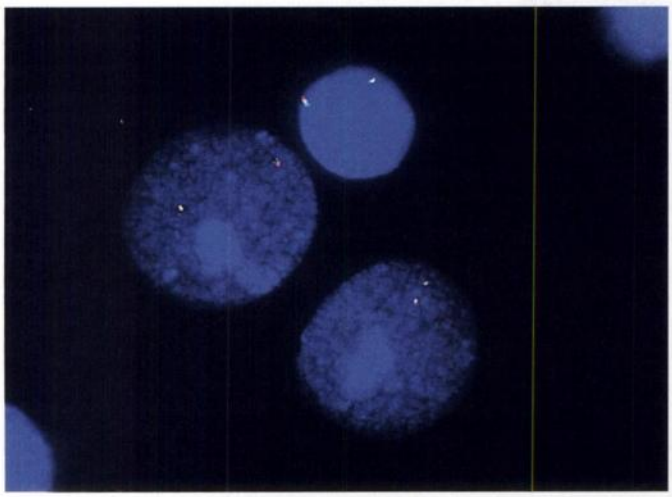

Fig. 2. Interphase FISH. Analysis was performed as described in "Materials and Methods" using human interphase nuclei. Both signals for *hMSH2* (*green*) and *hMSH6* (*red*) are very close to each other or indistinguishable, indicating a short distance between both genes on chromosome 2p.

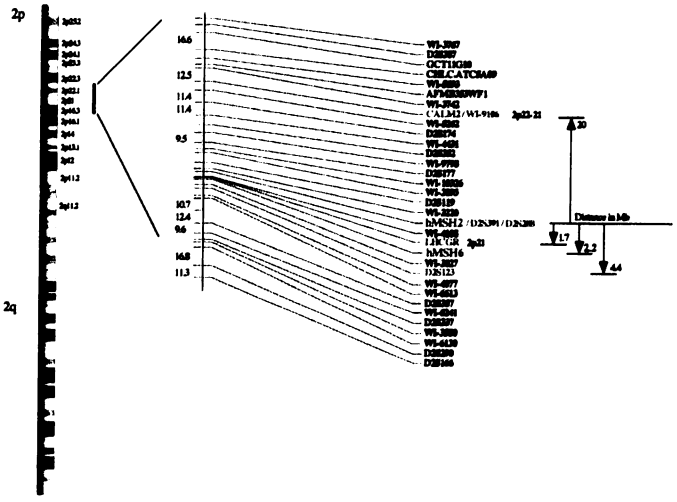

Fig. 3. Human chromosome 2. *CALM2*, *hMSH2*, *LHCGR*, *hMSH6*, and several markers (*red*) were mapped to chromosome 2p22–16.3 by the RH method. Distances were calculated assuming 270 kb per cR. *CALM2* and *LHCGR* have been mapped previously by FISH to 2p21 and 2p22–21, respectively (*green*; see text). Both *hMSH2* and *hMSH6* are located telomeric to marker D2S123, which was used in previous studies (see text).

Mouse Mapping. We have confirmed our initial mouse mapping analysis, which suggested that *Msh2* was also located telomeric to the *LHCGR* gene on mouse chromosome 17 in the region of synteny with human chromosome 2p22–21. To further define this locus, we determined the mouse chromosomal location of *Msh6* by similar interspecific backcross analysis using progeny derived from matings of [(C57BL/6J × *M. spretus*)F_1 × C57BL/6J] mice. This interspecific backcross mapping panel has been typed for over 2500 loci that are well distributed among all of the autosomes, as well as the X chromosome (26). C57BL/6J and *M. spretus* DNAs were digested with several enzymes and analyzed by Southern blot hybridization for informative RFLPs using a human cDNA probe. The 5.4- and 2.5-kb *Taq*I *M. spretus* RFLPs (see "Materials and Methods") were used to follow the segregation of the *Msh6* locus in backcross mice. The mapping results indicate that *Msh6* was located in the distal region of the mouse chromosome 17 linked to *Tik*, *Sos1*, *Msh2*, and *Lhcgr*. Although 155 mice were analyzed for every marker and are shown in the segregation analysis (Fig. 4), up to 191 mice were typed for some pairs of markers. Each locus was analyzed in pairwise combinations for recombination frequencies using the additional data. The most likely gene order is (the ratios of the total number of mice exhibiting recombinant chromosomes to the total number of mice analyzed for each pair of loci are shown in parentheses): centromere-*Tik* (1/162)-*Sos1* (3/158)-*Msh6* (0/189)-*Msh2* (1/191)-*Lhcgr*. The recombination frequencies [expressed as genetic distances (in cM) ± SE] are: *Tik*, 0.6 ± 0.6; *Sos1*, 1.9 ± 1.1; *Msh6* and *Msh2*, 0.5 ± 0.5; *Lhcgr*. No recombinants were detected between *Msh2* and *Msh6* in 189 animals with common types, suggesting that the two loci are within 1.6 cM of each other (upper 95% confidence limit). These data suggest that the genomic positions of *Msh2* and *Msh6* in mouse are indistinguishable from each other.

It is interesting to note that the human RH analysis places *LHCGR* between *hMSH2* and *hMSH6*, whereas the mouse mapping studies place *LHCGR* centromeric to both *hMSH2* and *hMSH6*. These results may suggest that the resolution of the RH map is insufficient to distinguish *hMSH6* and *LHCGR* or that a small interstitial rearrangement has occurred during the evolution of mouse and humans.

We have compared our interspecific map of chromosome 17 with a composite mouse linkage map that reports the map location of many uncloned mouse mutations (provided from Mouse Genome Database,

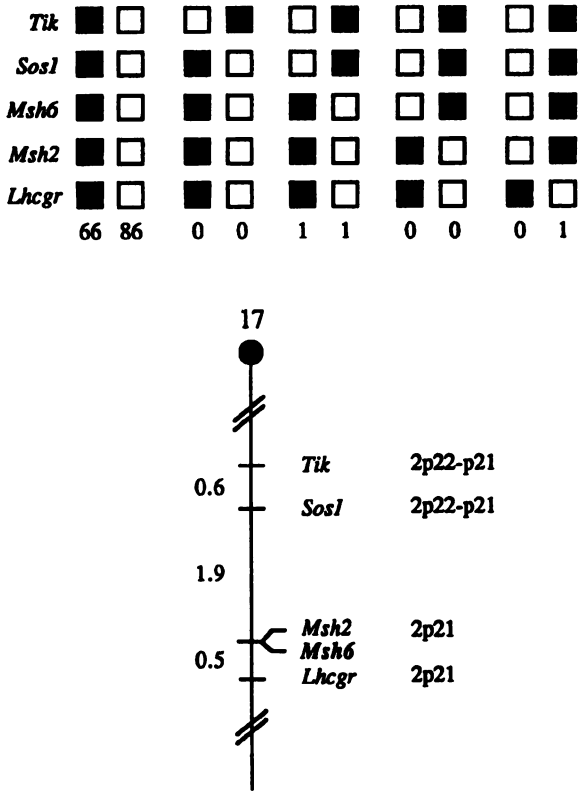

Fig. 4. Mapping in mouse. *Msh6* maps in the distal region of mouse chromosome 17. *Msh6* was placed on mouse chromosome 17 by interspecific backcross analysis. The segregation patterns of *Msh6* and flanking genes in 155 backcross animals that were typed for all loci are shown at the top of the figure. For individual pairs of loci, more than 155 animals were typed (see text). Each column represents the chromosome identified in the backcross progeny that was inherited form the (C57BL/6J × *M. spretus*)F_1 parent. ■, presence of a C57BL/6J allele; □, presence of a *M. spretus* allele. The number of offspring inheriting each type of chromosome is listed at the bottom of each column. A partial chromosome 17 linkage map showing the location of *Msh6* in relation to linked genes is shown at the bottom of the figure. Recombination distances between loci in cM are shown to the *left* of the chromosome, and the position of loci in human chromosomes, if known, are shown to the *right*. References for the human map position of loci cited in this study can be obtained from Genome Database, a computerized database of human linkage information maintained by The William H. Welch Medical Library of The Johns Hopkins University (Baltimore, MD).

a computerized database maintained at The Jackson Laboratory, Bar Harbor, ME). *Msh6* mapped in a region of the composite map that lacks mouse mutations with a phenotype that might be expected for an alteration in this locus (data not shown).

Conclusion. In summary, these combined data confirm our original conclusion that *hMSH2* maps to chromosome 2p21. *hMSH6* appears to map closer to the 2p16.3 border (2p21–16.3). This high-resolution mapping of several markers surrounding this genomic locus by FISH and relative to the RH grid should be useful in linkage and chromosomal studies of HNPCC families or other tumors showing MSI.

Acknowledgments

The authors thank Hans-Jürg Alder and the Kimmel Nucleic Acids Facility for oligonucleotide synthesis and Debra J. Gilbert for excellent technical assistance.

References

1. Lindahl, T. Instability and decay of the primary structure of DNA. Nature (Lond.), *362:* 709–715, 1993.
2. Spruck, C. H., Rideout, W. M., and Jones, P. A. DNA methylation and cancer. *In:* J. P. Jost and H. P. Saluz (eds.), DNA Methylation: Molecular Biology and Biological Significance, pp. 487–509. Basel: Birkhäuser Verlag, 1993.
3. Sweezy, M. A., and Fishel, R. Multiple pathways leading to genomic instability and tumorigenesis. *In:* S. S. Wallace, B. Van Houten, and Y. W. Kow (eds.), DNA Damage: Effects on DNA Structure and Protein Recognition, Vol. 726, pp. 165–177. New York: The New York Academy of Sciences, 1994.
4. Su, S. S., and Modrich, P. *Escherichia coli* mutS-encoded protein binds to mismatched DNA base pairs. Proc. Natl. Acad. Sci. USA, *83:* 5057–5061, 1986.
5. Lahue, R. S., Au, K. G., and Modrich, P. DNA mismatch correction in a defined system. Science (Washington DC), *245:* 160–164, 1989.
6. Demerec, M., Lahr, E. L., Miyake, T., Galehran, E., Balbinder, E., Baric, S., Hashimoto, K., Glanville, E. V., and Gross, J. D. Bacterial genetics. Carnegie Inst. Wash. Yearbook, *370:* 390–406, 1957.
7. Miyake, T. Mutator factor in *Salmonella typhimurium*. Genetics, *45:* 755–762, 1960.
8. Siegel, E. C., and Bryson, V. Mutator gene of *Escherichia coli* B. J. Bacteriol., *94:* 38–47, 1967.
9. Siegel, E. C. Genetic location in *Escherichia coli* K-12 of the ultraviolet-sensitive mutation uvrD3. J. Bacteriol., *104:* 604–605, 1970.
10. Hill, R. F. Location of genes controlling excision repair of UV damage and mutator activity in *Escherichia coli* WP2. Mutat. Res., *9:* 341–344, 1970.
11. Fishel, R., and Wilson, T. MutS homologs in mammalian cells. Curr. Opin. Genet. Dev., *7:* 105–113, 1997.
12. Marsischky, G. T., Filosi, N., Kane, M. F., and Kolodner, R. Redundancy of *Saccharomyces cerevisiae* MSH3 and MSH6 in MSH2-dependent mismatch repair. Genes Dev., *10:* 407–420, 1996.
13. Alani, E. The *Saccharomyces cerevisiae* Msh2 and Msh6 proteins form a complex that specifically binds to duplex oligonucleotides containing mismatched DNA base pairs. Mol. Cell. Biol., *16:* 5604–5615, 1996.
14. Acharya, S., Wilson, T., Gradia, W., Kane, M. F., Guerette, S., Marsischky, G., Kolodner, R., and Fishel, R. hMSH2 forms specific mispair-binding complexes with hMSH3 and hMSH6. Proc. Natl. Acad. Sci. USA, *93:* 13629–13634, 1996.
15. Fishel, R., Lescoe, M. K., Rao, M. R. S., Copeland, N. G., Jenkins, N. A., Garber, J., Kane, M., and Kolodner, R. The human mutator gene homolog *MSH2* and its association with hereditary nonpolyposis colon cancer. Cell, *75:* 1027–1038, 1993.
16. Peltomäki, P., and Vasen, H. F. Mutations predisposing to hereditary nonpolyposis colorectal cancer: database and results of a collaborative study. The International Collaborative Group on Hereditary Nonpolyposis Colorectal Cancer. Gastroenterology, *113:* 1146–1158, 1997.
17. Peinado, M. A., Malkhosyan, S., Velazquez, A., and Perucho, M. Isolation and characterization of allelic losses and gains in colorectal tumors by arbitrarily primed polymerase chain reaction. Proc. Natl. Acad. Sci. USA, *89:* 10065–10069, 1992.
18. Ionov, Y., Peinado, M. A., Malkhosyan, S., Shibata, D., and Perucho, M. Ubiquitous somatic mutations in simple repeated sequences reveal a new mechanism for colonic carcinogenesis. Nature (Lond.), *363:* 558–561, 1993.
19. Peltomäki, P., Lothe, R. A., Aaltonen, L. A., Pylkkänen, L., Nyström-Lahti, M., Seruca, R., David, L., Holm, R., Ryberg, D., Haugen, A., Brøgger, A., Børresen, A-L., and de la Chapelle, A. Microsatellite instability is associated with tumors that characterize the hereditary non-polyposis colorectal carcinoma syndrome. Cancer Res., *53:* 5853–5855, 1993.
20. Aaltonen, L. A., Peltomäki, P., Leach, F. S., Sistonen, P., Pylkkänen, L., Mecklin, J. P., Järvinen, H., Powell, S. M., Jen, J., Hamilton, S. R., Petersen, G. M., Kinzler, K. W., and Vogelstein, B. Clues to the pathogenesis of familial colorectal-cancer. Science (Washington DC), *260:* 812–816, 1993.
21. Liu, B., Parsons, R., Papadopoulos, N., Nicolaides, N. C., Lynch, H. T., Watson, P., Jass, J. R., Dunlop, M., Wyllie, A., Peltomäki, P., de la Chapelle, A., Hamilton, S. R., Vogelstein, B., and Kinzler, K. W. Analysis of mismatch repair genes in hereditary non-polyposis colorectal cancer patients. Nat. Med., *2:* 169–174, 1996.
22. Peltomäki, P., Aaltonen, L. A., Sistonen, P., Pylkkänen, L., Mecklin, J. P., Järvinen, H., Green, J. S., Jass, J. R., Weber, J. L., Leach, F. S., Petersen, G. M., Hamilton, S. R., de la Chapelle, A., and Vogelstein, B. Genetic mapping of a locus predisposing to human colorectal cancer. Science (Washington DC), *260:* 810–812, 1993.
23. Leach, F. S., Nicolaides, N. C., Papadopoulos, N., Liu, B., Jen, J., Parsons, R., Peltomäki, P., Sistonen, P., Aaltonen, L. A., Trent, J. M., de la Chapelle, A., Kinzler, K. W., and Vogelstein, B. Mutations of a mutS homolog in hereditary nonpolyposis colorectal cancer. Cell, *75:* 1215–1225, 1993.
24. Green, R. C., Narod, S. A., Morasse, J., Young, T. L., Cox, J., Fitzgerald, G. W., Tonin, P., Ginsburg, O., Miller, S., Jothy, S., and Rousseau, F. Hereditary nonpolyposis colon cancer: analysis of linkage to 2p15–16 places the *COCA1* locus telomeric to D2S123 and reveals genetic heterogeneity in seven Canadian families. Am. J. Hum. Genet., *54:* 1067–1077, 1994.
25. Hudson, T., Stein, L., Gerety, S., Ma, J., Castle, A., Silva, J., Slonim, D., Baptista, R., Kruglyak, L., Xu, S., Hu, X., Colbert, A., Rosenberg, C., Reeve-Daly, M., P., Rozen, S., Hui, L., Wu, X., Vestergaard, C., Wilson, K., Bae, J., Maitra, S., Ganiatsas, S., Evans, C., DeAngelis, M., Ingalls, K., Nahf, R., Horton, L., Oskin, M., Collymore, A., Ye, W., Kouyoumjian, V., Zemsteva, I., Tam, J., Devine, R., Courtney, D., Renaud, M., Nguyen, H., O'Connor, T., C., F., Faure, S., Gyapay, G., Dib, C., Morissette, J., Orlin, J., Birren, B., Goodman, N., Weissenbach, J., Hawkins, T., Foote, S., Page, D., and Lander, E. An STS-based map of the human genome. Science (Washington DC), *270:* 1945–1954, 1995.
26. Copeland, N. G., and Jenkins, N. A. Development and applications of a molecular genetic linkage map of the mouse genome. Trends Genet., *7:* 113–118, 1991.
27. Jenkins, N. A., Copeland, N. G., Taylor, B. A., Bedigian, H. G., and Lee, B. K. Ecotropic murine leukemia virus DNA content of normal and lymphomatous tissues of BXH-2 recombinant inbred mice. J. Virol., *42:* 379–388, 1982.
28. Carey, A. H. Use of commercially available radiation hybrid panels. *In:* Current Protocols in Human Genetics, pp. 3.5.1–3.5.10. New York: John Wiley & Sons, Inc., 1997.
29. Boehnke, M., Lange, K., and Cox, D. R. Statistical methods for multipoint radiation hybrid mapping. Am. J. Hum. Genet., *49:* 1174–1188, 1991.
30. Papadopoulos, N., Nicolaides, N. C., Liu, B., Parsons, R., Lengauer, C., Palombo, F., Darrigo, A., Markowitz, S., Willson, J. K. V., Kinzler, K. W., Jiricny, J., and Vogelstein, B. Mutations of GTBP in genetically unstable cells. Science (Washington DC), *268:* 1915–1917, 1995.
31. Berchtold, M. W., Egli, R., Rhyner, J. A., Hameister, H., and Strehler, E. E. Localization of the human bona fide calmodulin genes *CALM1*, *CALM2*, and *CALM3* to chromosomes 14q24–q31, 2p21.1–p21.3, and 19q13.2–q13.3. Genomics, *16:* 461–465, 1993.
32. Rousseau-Merck, M. F., Misrahi, M., Atger, M., Loosfelt, H., Milgrom, E., and Berger, R. Localization of the human luteinizing hormone/choriogonadotropin receptor gene (*LHCGR*) to chromosome 2p21, Cytogenet. Cell Genet., *54:* 77–79, 1990.